Sum Rate and Max-Min Rate for Cellular-Enabled UAV Swarm Networks

Bin Yang, Yongchao Dang, Tarik Taleb, Shikai Shen, and Xiaohong Jiang

***Abstract*—This paper investigates the fundamental rate performances in the highly promising cellular-enabled unmanned aerial vehicle (UAV) swarm networks, which can provide ubiquitous wireless connectivity for supporting various Internet of things (IoT) applications. We first provide the formulations for the sum rate maximization and max-min rate, which are two nonlinear optimization problems subject to the constraints of UAV transmit power and antenna parameters at base station (BS). For the sum rate maximization problem, we propose an iterative algorithm to solve it utilizing the Karush–Kuhn–Tucker (KKT) condition. For the max-min rate problem, we transform it to an equivalent conditional eigenvalue problem based on the nonlinear Perron-Frobenius theory, and thus design an iterative algorithm to obtain the solution of such problem. Finally, numerical results are presented to indicate the effect of some key parameters on the rate performances in such networks.**

***Index Terms*—Directional antennas, IoT, performance optimization, power control, UAV networks.**

I. Introduction

UNMANNED aerial vehicle (UAV) networks, which enable each UAV to communicate directly with nearby UAVs and user equipments (UEs) via wireless channel, are envisioned to be an essential component of next generation (5 G) and beyond wireless networks [1], [2]. The UAV networks have many remarkable advantages like high flexibility, cost-effective and swift deployment, line-of-sight (LoS) dominant links, and thus have been widely used in various Internet of things (IoT) applications like precision agriculture, video streaming, surveillance, remote sensing, etc. [3], [4], [5], [6], [7]. However, most of available UAV networks perform simple point-to-point communication over unlicensed spectrum (e.g.,industrial scientific medical band at 2.4 GHZ). Therefore, such networks have low rate, unreliability, insecurity, and limited LoS communication range. These limitations are hindering their large-scale deployment.

To realize their widespread deployment, it is critical to guarantee that the UAV networks have high-rate, reliable and secure communication links and each UAV in such networks has ability to timely send information to distant UEs for supporting various applications [8], [9]. A promising solution is to integrate UAVs into the cellular networks forming a new cellular-enabled UAV networks, where UAVs as flying UEs can utilize licensed spectrum of cellular networks and ubiquitous ground base stations (BSs) to achieve substantial performance improvement in terms of rate, reliability, security and coverage, and also to provide high data rate communications with distant UEs from thousands of kilometers away, compared to the traditional UAV networks operated over the unlicensed spectrum.

The performance studies are of great importance to support various applications of the UAV networks. The existing works on the UAV networks mainly investigate the performances of rate, sum rate, max-min rate, coverage and energy efficiency under the scenario, where UAVs serve as either flying BSs or UEs without the support of ground BSs. The results in these works illustrate that the performances are improved by optimizing the following different system parameters: UAV trajectory or UAV placement [10], [11], [12], UAV height [13], joint UAV trajectory and power assignment [14], [15], joint UAV trajectory and communication scheduling [16], joint UAV height and antenna beamwidth [17], joint UAV trajectory, communication scheduling and power assignment [18], joint UAV trajectory, bandwidth and power assignment [19], joint UAV trajectory, communication time assignment and mission completion time [20], joint UAV height, antenna beamwidth, power and bandwidth assignment [21], and joint UAV trajectory, power assignment, communication scheduling and association [22].

However, there are only some initial works on the new cellular-enabled UAV networks [23], [24], [25], [26], [27], [28], [29], [30]. Such works are devoted to the investigation of performances in term of rate, sum rate, coverage, mission completion time, secrecy rate, and covert rate by setting different parameters such as UAV cache size and density [23], UAV

Manuscript received 23 February 2022; revised 16 June 2022; accepted 8 August 2022. Date of publication 6 September 2022; date of current version 16 January 2023. This work was supported in part by the National Natural Science Foundation of China under Grant 61962033, in part by the Academy of Finland Projects: 6Genesis under Grant 318927 and IDEA-MILL under Grant 335936, and in part by the Natural Science Project of Anhui/Chuzhou University under Grants 2020qd16, KJ2021ZD0128, KJ2021ZD0129, and 2022XJZD12. The review of this article was coordinated by Prof. Chadi Assi. *(Corresponding author: Shikai Shen.)*

Bin Yang is with the School of Computer and Information Engineering, Chuzhou University, Chuzhou 239000, China, and also with the School of Information and Technology, Kunming University, Kunming 650208, China (e-mail: yangbinchi@gmail.com).

Yongchao Dang is with the Department of Communications and Networking, School of Electrical Engineering, Aalto University, 02150 Espoo, Finland (e-mail: yongchao.dang@aalto.fi).

Tarik Taleb is with the Information Technology and Electrical Engineering, University of Oulu, 90570 Oulu, Finland, and also with the Department of Computer and Information Security, Sejong University, Seoul 143-747, South Korea (e-mail: talebtarik@gmail.com).

Shikai Shen is with the School of Information and Technology, Kunming University, Kunming 650208, China (e-mail: kmssk2000@sina.com).

Xiaohong Jiang is with the School of Systems Information Science, Future University Hakodate, Hakodate 041-8655, Japan (e-mail: jiang@fun.ac.jp).

Digital Object Identifier 10.1109/TVT.2022.3204624

trajectory design [24], spectrum resource allocation [29], jamming node selection [30], joint power assignment of BSs and beamforming [25], joint UAV speed and channel assignment [26], joint uplink cell association of UAV and power assignment [27], and joint power and UAV placement [28]. In particular, power assignment and bemforming are two important solutions to improve the network performance in the above works. The increasing of transmit power can enhance the received signal strength but also cause severely interference among the links using the same spectrum, while beamforming technique can significantly mitigate the interference. Note that power assignment and beamforming in [27] are adopted in an uplink transmission scenario with a UAV. The joint power assignment and beamforming are further considered in a downlink transmission scenario, where UAVs and BSs have a single antenna and directional antenna array, respectively [25]. Note that the directional antenna array using beamforming are ideal that the array gain is considered to be a fixed value when radiation angles is in the beamwidth, and small value or zero outside [25], [27]. Actually, the gain is strong angle-dependent [31]. Recently, we explore the performances of millimeter wave (mmWave) cellular-enabled UAV swarm networks with angle-dependent directional antennas, where the performance metrics include sum-rate, fairness index, max-min rate and proportional fairness [32]. In the work, the UAVs and BS employ fixed transmit power to communicate with each other at mmWave bands. However, it is still unknown how to jointly optimize UAV transmit power and beamforming of antenna array for improving the performances in the traditional cellular-enabled UAV swarm networks operated at sub-6 GHZ bands, which therefore is quite challenging and of great importance.

Motivated by this observation, this paper studies fundamental rate performances by jointly optimizing the power assignment and beamforming in uplink transmission cellular-enabled UAV swarm networks with sub-6 GHZ bands, where each UAV and BS are equipped more realistic directional antenna array with variable array gain. We first maximize the sum rate of the networks. This may lead to unfair rate assignment such that the worse-case links have lower rates. To satisfy different requirements for rate performances in future applications, the max-min rate is further explored to maximize the minimum rate which guarantees the rate fairness among links in the networks. To the best of our knowledge, this work is the first effort to comprehensively study the rate performances by jointly optimizing the power assignment and the array parameters (i.e.,the array elevation angle, the azimuth angle and height) associated with beamforming in the cellular-enabled UAV swarm networks. The main contributions are summarized as follows.

- We consider a more realistic antenna array to characterize the three dimensional antenna beamforming gain in cellular-enabled UAV swarm networks. In the uplink transmission networks, we first formulate the sum rate maximization as an optimization problem subject to the constraints of transmit power and the antenna parameters at BS. We propose an iterative algorithm for solving the problem utilizing the Karush–Kuhn–Tucker (KKT) conditions.
- We formulate the max-min rate as a constrained optimization problem in the uplink transmission scenario. To solve the nonlinear optimization problem, we first convert it to an equivalent conditional eigenvalue problem of nonlinear Perron-Frobenius theory, and then propose an iterative algorithm for solving the problem utilizing the theory.
- Finally, extensive numerical results are presented to indicate the effect of system parameters on the sum rate, minimum rate and fairness index, and also to show our new findings.

The remainder of the paper is structured as follows. Section II reviews the related works. The system model is introduced in Section III. The problem formulations and solutions of these two problems are presented in Sections IV and V, respectively. Section VI provides the numerical results. Finally, Section VII concludes the paper.

This paper will use the following notations. For any two vectors $\mathbf{a} = [a_1, \ldots, a_m]^{\mathrm{T}}$ and $\mathbf{b} = [b_1, \ldots, b_m]^{\mathrm{T}}$ with length m, we say that $\mathbf{a} > \mathbf{b}$ if $a_i > b_i$, for all i; $\mathbf{a} \leq \mathbf{b}$ if $a_i \leq b_i$, for all i, but $\mathbf{a} \neq \mathbf{b}$; and $\mathbf{a} \leqq \mathbf{b}$ if $a_i \leq b_i$, for all i.

II. Related Works

In the UAV networks, the available works on the performance studies mainly consider two scenarios with/without the support of ground BSs.

1) UAV networks without BS: Many efforts have been devoted to investigating the performances of such networks such as rate, sum rate, max-min rate, coverage and energy efficiency. Regarding the rate performances, the authors in [14] jointly optimize source/relay power assignment and relay trajectory to maximize the rate from source to destination in a UAV network including a fixed source-destination pair and a mobile UAV relay. By jointly optimizing the UAV height and antenna beamwidth, the work in [17] aims at maximizing the sum rate of a UAV network, where a flying UAV BS equipped with a directional antenna serves multiple ground UEs. Later, the sum rate maximization is studied via a joint optimization of UAV trajectory and power assignment in a multi-UAV network, where multiple UAVs are associated with ground UEs [15]. The work in [18] considers simultaneous uplink and downlink transmission networks, where one UAV sends data to multiple access points (APs), and another UAV as a flying BS collects data from ground sensor nodes (SNs). The sum rate maximization is achievable via a joint optimization of the UAV trajectory, communication scheduling, and UAV AP/SN power assignment. By deploying a UAV as a flying BS to assist a group of ground UEs, the work in [19] aims at maximizing the minimum rate via a joint optimization of the UAV trajectory, bandwidth and power assignment in a UAV-assisted orthogonal frequency-division multiple access network. The authors in [16] maximizes the minimum average data collection rate from all SNs by a joint optimization of the UAV trajectory and communication scheduling under more practically accurate angle-dependent Rician fading channels. The max-min rate optimization problem is studied by a joint optimization of UAV height, antenna beamwidth, power and bandwidth assignment for ground UEs in a UAV network

including a group of ground UEs and a single-antenna UAV as a flying BS using nonorthogonal multiple access [21]. The work in [22] deploys multiple UAVs as flying BSs to assist a group of ground UEs, and then explores the max-min rate performance by a joint optimization of the UAV trajectory, power assignment, multiuser communication scheduling and association.

Regarding the performances of coverage, energy and completion time in such networks, a general framework is developed to explore the coverage probability performance of a reference ground receiver using stochastic geometry [13]. In this study, UAVs are assumed to be uniformly distributed in a finite area forming a uniform binomial point process. To provide full wireless coverage of UAVs over a target area, the author in [10] studies two fast UAV deployment schemes: minimizing the maximum deployment delay among all UAVs and minimizing the total deployment delay. For the energy performance, the authors in [11] optimize the UAV trajectory to maximize the energy efficiency in a UAV network, where a UAV sends information to a ground UE, and the energy efficiency is defined as the total rate divided by the total UAV propulsion energy consumed. The work of [11] is further extended to the scenario with a UAV and multiple ground UEs, and the total energy consumption is minimized by a joint optimization of the UAV trajectory, communication time assignment among ground UEs and the total mission completion time [20]. The mission completion time is minimized by optimizing the UAV trajectory in a UAV-enabled multicasting network, where a UAV sends a common file to a group of ground UEs [12].

2) Cellular-enabled UAV networks: For the rate performances, the work in [25] jointly optimizes the power assignment of BSs and beamforming to maximize the rate from BS to UAV using a divide-and-conquer approach in a downlink cellular-enable UAV network, where the ground BSs serve multiple UAVs and ground UEs, each UAV employs a single antenna, and each BS is equipped with an antenna array with fixed directional gain. By jointly optimizing the UAV's cell association and power assignment, the work of [27] aims to maximize the weighted sum rate of the UAV and ground UEs in an uplink transmission cellular-enabled UAV network consisting a UAV, a set of ground UEs and multiple BSs. With the help of a UAV relay, the sum rate is maximized by optimizing power assignment of each ground UE and UAV placement in the network with a UAV, multiple ground UEs and BSs [28]. By deploying multiple UAVs, UEs and a BS, the objective of [26] is to jointly optimize UAV speed and channel assignment to maximize uplink sum rate. The work in [23] indicates that the coverage performance can be improved by properly setting UAV cache size and density in a cellular-enabled UAV network. The work in [24] further indicates that a minimum UAV's mission completion time is achievable by optimizing its trajectory in such a network. The authors in [29] propose a spectrum sharing strategy to utilize interference caused by spectrum reuse for enhancing secrecy rate performance in cellular-enabled UAV networks. Recently, the authors in [30] further propose a cooperative jamming strategy for improving covert performance in terms of covert rate and detection error probability in such networks, where under the cooperative jamming, the idle D2D pairs can send artificial noise to confuse the detection of adversaries.

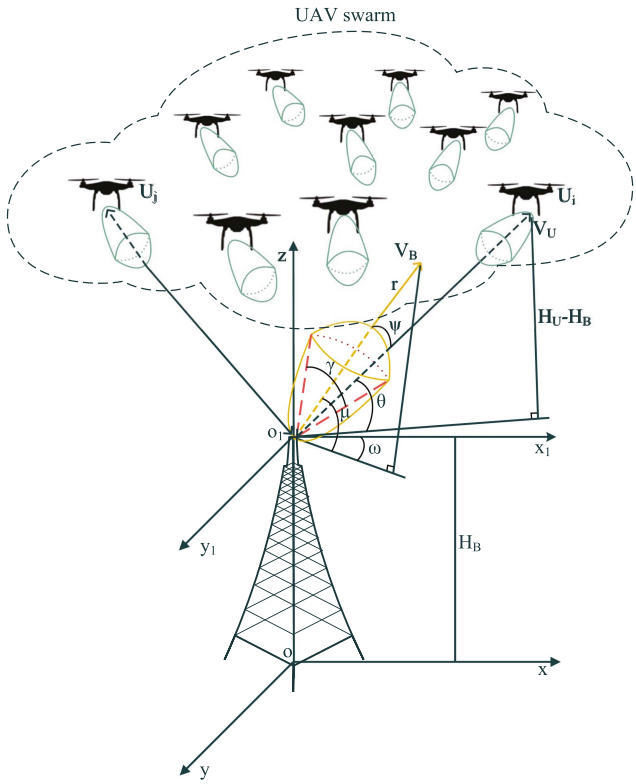

Fig. 1. A cellular-enabled UAV swarm network model.

III. System Models

A. Network Model

We consider an uplink cellular-enabled UAV swarm network including a BS and a rotary-wing UAV swarm as shown in Fig. 1. These UAVs have high manoeuvrability because they can hover in a stationary position with the height H_U, take off and land vertically, and also fly in any direction. Such UAVs have been widely used in various fields such as monitoring traffic flow and fire, and providing local area communication services. The locations' distribution of these UAVs follows an independent homogeneous Poisson point process (PPP) Φ with intensity λ_U.

B. Directional Beamforming

As illustrated in Fig. 1, all UAVs and BS are equipped with antenna array for directional data transmission via beamforming operation. Suppose that the main beam of the array at each UAV is directed towards the BS such that the antenna gain keeps unchanged at a maximum value K_M^U. Since the side beam emits smaller power than the main beam, we consider the side beam gain at the BS is a small value K_S^B, while the main beam gain depends on the antenna boresight direction. According to [33], the main beam gain $K_M^B(\psi)$ at the BS is expressed as

$$K_M^B(\psi) = S_0(\tau)\cos(\psi), \tag{1}$$

where τ and $S_0(\tau)$ denote a directivity parameter and corresponding maximum value, respectively. We use ψ and $\cos(\psi)$ to denote the antenna radiation angle and radiation efficiency between boresight direction and radiation one, respectively. As shown in Fig. 1, $\overrightarrow{o_1V_B}$ denotes the boresight direction vector and $\overrightarrow{o_1V_U}$ denotes the radiation vector from the antenna position of the BS to a UAV U_i. Note that the main beam gain $K_M^B(\psi)$ exhibits a symmetric feature along $\overrightarrow{o_1V_B}$, and varies with these two parameters τ and ψ.

Regarding the two unknown items $S_0(\tau)$ and ψ in formula (1), the $S_0(\tau)$ is given by

$$S_0(\tau) = \frac{4\pi}{\Upsilon_A(\tau)}. \tag{2}$$

Based on [34], we further determine the $\Upsilon_A(\tau)$ as

$$\begin{aligned}\Upsilon_A(\tau) &= \int_0^{2\pi}\int_0^{\pi} U_\tau(\psi)\sin(\psi)d\psi d\omega,\\ &= \int_0^{2\pi}\int_0^{\frac{\pi}{2}} \frac{\cos(\psi)}{\tau}\sin(\psi)d\psi d\omega,\\ &= \frac{\pi}{2\tau}.\end{aligned} \tag{3}$$

In this formula, $U_\tau(\psi) = \cos(\psi)/\tau$ represents the normalized antenna radiation intensity. Because the back beam antenna gain is negligible, we omit the effect of back beam, i.e., $U_\tau(\psi) = 0$ when $\pi \geq |\psi| \geq \pi/2$. The main beam antenna gain equals to half of the maximum antenna directivity gain which is achievable when $\psi = \gamma/2$ such that $U_\tau(\gamma/2) = 0.5$. Here, γ represents the half-power beamwidth. Thus, we obtain

$$\gamma = 2\arccos(0.5\tau), \tag{4}$$

where $2 > \tau > 0$. According to these two formulas (2) and (3), we know that a bigger τ could result in a bigger antenna directivity corresponding to a smaller beamwidth, which means that the antenna main beam has a smaller coverage range.

We proceed to determine the antenna radiation angle ψ. Based on the dot product operation, ψ illustrated in Fig. 1 can be determined as

$$\psi = \arccos\frac{\overrightarrow{o_1V_B}\cdot\overrightarrow{o_1V_U}}{|\overrightarrow{o_1V_B}||\overrightarrow{o_1V_U}|}. \tag{5}$$

Here, the dot $\cdot$ represents the notation of dot product operation, and $|\overrightarrow{o_1V_B}|$ represents the square root of a vector $\overrightarrow{o_1V_B}$. The point $o_1 = (0, 0, H_B)$ denotes a three-dimensional coordinate of the antenna position equipped at the BS, where H_B denotes the height of the BS. The intersection point between $\overrightarrow{o_1V_B}$ and a sphere with radius r and center o_1 is denoted as $V_B = (r\cos\mu\cos\omega, r\cos\mu\sin\omega, r\sin\mu + \mathrm{H_B})$. The position coordinate of UAV U_i is denoted as $V_U = (x_U, y_U, H_U)$. Then, we have $\overrightarrow{o_1V_B} = (r\cos\mu\cos\omega, r\cos\mu\sin\omega, r\sin\mu)$ and $\overrightarrow{o_1V_U} = (x_U, y_U, H_U - H_B)$.

C. Channel Model

Since UAVs hover in the air, the channels from UAVs to BS probably exhibit the LoS characteristic. Thus, we consider the channels for UAV communications belong to the LoS links. However, this can also be extended to the situation non-line-of-sight (NLoS) links, as long as we multiply the received power of each NLoS link by an additional attenuation factor. A general Nakagami-m fading and power law path loss are used to model the LoS links. When a UAV i transmits information to the BS, the received power R_i of the BS can be expressed as

$$R_i = P_i K^B(\psi_i) K_M^U h_i |L_i|^{-\alpha}, \tag{6}$$

where P_i is the transmit power of the UAV no more than the maximum one P_m, h_i is the fading coefficient of current link from the UAV i to the BS, which follows a Nakagam-m distribution with parameter m, $|L_i|$ is the link distance, α is the path loss exponent, and $K^B(\psi_i)$ is the antenna gain with radiation angle ψ_i. The antenna gain can be determined as

$$K^B(\psi_i) = \begin{cases} K_M^B(\psi_i) & \text{if } 0 \leq \psi_{\mathrm{i}} \leq \gamma, \\ K_S^B & \text{if } \psi_{\mathrm{i}} > \gamma. \end{cases} \tag{7}$$

We assume that the network has N orthogonal equal-sized resource blocks, each of which corresponds to a channel with bandwidth W MHZ. Each UAV is randomly assigned to a channel for information transmission. There exists mutual interference among the UAVs using the same channel. On the other hand, interference does not occur among the UAVs reusing different orthogonal channels. Furthermore, we consider the additive white Gaussian noise as channel one with variance σ^2.

D. Link Rate

According to the above the network model, directional beamforming operation and channel model, we can calculate the LoS link rate from UAV i to the BS as

$$\Re_i = W\log_2(1 + \mathrm{SINR}_i(\mathbf{P}, \mu, \omega, H_B)). \tag{8}$$

where $\Re_i$ denotes the link rate, $\mathbf{P} = [P_1, \ldots, P_{|\Phi|}]^{\mathrm{T}}$ denotes a vector of transmit power, any element P_i denotes the transmit power of UAV i, and $|\Phi|$ represents the number of UAVs in our concerned network. Here, the signal-to-interference-plus-noise ratio (SINR) received from a UAV i at the BS can be given by

$$\mathrm{SINR}_i(\mathbf{P}, \mu, \omega, H_B) = \frac{R_i}{I_i + \sigma^2}, \tag{9}$$

where the interference from other UAVs except UAV i received by the BS is denoted as I_i. We further determine I_i as

$$I_i = \sum_{j\in\Phi_i^*, j\neq i} P_j K^B(\psi_j) K_M^U h_j |L_j|^{-\alpha}, \tag{10}$$

where the set Φ_i^* consists of UAVs reusing the same channel as UAV i.

IV. Problem Formulation and Solution of Sum Rate Maximization

To deal with the sum rate maximization problem, we first formulate it as a constrained optimization problem, and present an iterative algorithm to solve this optimization problem.

A. Problem Formulation

The sum rate maximization aims to jointly optimize the transmit power of each UAV and various antenna parameters for maximizing sum rate of the concerned network, which can be formulated as the following constrained optimization problem.

$$\max_{\mu,\omega,H_B,\mathbf{P}} \sum_{i\in\Phi} \Re_i, \tag{11a}$$

$$s.t. \quad 0 \le \mu \le \pi, \tag{11b}$$

$$0 \le \omega \le 2\pi, \tag{11c}$$

$$0 \le H_B \le H_{\max}, \tag{11d}$$

$$0 \le P_i \le P_{\max}, \tag{11e}$$

where $P_{\max}$ is the maximum transmit power for each UAV, and $H_{\max}$ is the maximum antenna height. Constraints (11b), (11c) and (11d) define the range of the antenna parameters such as the elevation angle μ, azimuth angle ω and antenna height H_B, and constraint (11e) gives the range of the transmit power for any UAV i.

B. Solution of Sum Rate Maximization

The following Lemma 1 illustrates that the (11) is a concave optimization problem.

Lemma 1: For each fixed setting of μ, ω and H_B, the objective function of (11a) with power constraint of (11e) is a concave optimization problem.

Proof: Since each item (i.e., $\Re_i$) in (11a) is a concave function, the second derivative of the item with respect to $\mathbf{P}$ is less than zero. Then, we know that the second derivative of (11a) is also less than zero. Thus, (11a) is a concave function of $\mathbf{P}$, and then the Lemma 1 follows. ■

Using the KKT conditions for the optimization problem in (11), we now can obtain a fixed point iteration written by $\mathbf{P} = f(\mathbf{P})$ for some function f. For the concave objective function in (11a), when the first derivation of (11a) equals to zero, we can obtain P_i.

$$P_i(\beta+1) = \min\{\mathrm{P_i}(\beta), \mathrm{P_{max}}\}, \tag{12}$$

where $P_i(\beta)$ denotes the value of P_i in the βth iteration.

Based on the above iteration equation, we further propose the following Algorithm 1 for solving the optimization problem.

Algorithm 1: Solution of Sum Rate Maximization.

1. **Input:** Given the values of the following parameters: H_U, W, K_S^B, K_M^U and σ^2.
2. **Output:** Maximum sum rate T_{m}.
3. Initialize $T_{\mathrm{m}} = 0$, $\beta = 0$, $P_i(\beta) = P_{max}$, and step size λ_μ, λ_ω and λ_H.
4. **for** $\mu = 0; \mu \le \pi; \mu = \mu + \lambda_\mu$ **do**
5. **for** $\omega = 0; \omega \le 2\pi; \omega = \omega + \lambda_\omega$ **do**
6. **for** $H_B = 0; H_B \le H_{max}; H_B = H_B + \lambda_H$ **do**
7. Repeat to update $P_i(\beta+1)$ of each UAV i utilizing (12) until convergence.
8. Calculate sum rate $\Re(\mathbf{P}(\beta+1))$ defined in (11a).
9. **if** $T_{\mathrm{m}} < \Re(\mathbf{P}(\beta+1))$ **then**
10. $T_{\mathrm{m}} = \Re(\mathbf{P}(\beta+1))$.
11. **end if**
12. **end for**
13. **end for**
14. **end for**

V. Problem Formulation and Solution of Max-Min Rate

This section first gives the problem formulation for the max-min rate, and then proposes an algorithm to solve the problem.

A. Problem Formulation

The goal of max-min rate is to maximize the minimum link rate, which ensures the rate allocation fairness among different links. It can be modeled as the following optimization problem.

$$\max_{\theta,\varphi,H_B,\mathbf{P}} \min_{i\in\Phi} \Re_i, \tag{13a}$$

$$s.t. \quad 0 \le \mu \le \pi, \tag{13b}$$

$$0 \le \omega \le 2\pi, \tag{13c}$$

$$0 \le H_B \le H_{\max}, \tag{13d}$$

$$0 \le P_i \le P_{\max}, \tag{13e}$$

where (13a) guarantees the fairness, and the constraints are the same as these of (11).

B. Solution of Max-Min Rate

The optimization problem of max-min rate in (13) is equivalent to maximizing an additional variable Z that is a lower bound for each rate. Thus, we have

$$\max_{\theta,\varphi,H_B,P_i} Z, \tag{14a}$$

$$s.t. \quad \Re_i \ge Z, \text{ for all } i$$

$$(13b), (13c), (13d) \text{ and } (13e). \tag{14b}$$

To solve it, we first give the follow Lemma.

Lemma 2: For each fixed setting of μ, ω and H_B, we denote by Z^* and $\mathbf{P}^*$ the optimal value and optimal solution of (14). We have that $Z^* > 0$, $\mathbf{P}^* > 0$ and when $\mathbf{P} = \mathbf{P}^*$, $\Re_i = Z^*$, for all $i \in \Phi$.

Proof: From (8), we know that when $\mathbf{P} > 0$, $\Re_i > 0$ and when $\mathbf{P} = 0$, $\Re_i = 0$. Since each UAV transmits message to the BS with transmit power $\mathbf{P} > 0$ satisfying the constraint of maximum transmit power P_{max}, we can obtain that the objective function in $(13a)$ is a positive value, i.e., $Z^* > 0$. Thus, both the optimal value Z^* and optimal solution $\mathbf{P}^*$ are two positive values.

Suppose that we can find some i, there are $\mathbf{P} = \mathbf{P}^*$ and $\Re_i > Z^*$, it implies that the optimization problem has an optimal value $Z = Z'$ more than Z^*. This contradicts that Z^* is optimal. Thus, when $\mathbf{P} = \mathbf{P}^*$, $\Re_i = Z^*$, for all $i \in \Phi$. ■

We define a vector $\mathbf{F}(\mathbf{P}^*) = [F_1(\mathbf{P}^*), \ldots, F_{|\Phi|}(\mathbf{P}^*)]^{\mathrm{T}}$, any element of which $F_i(\mathbf{P}^*) = \frac{P_i^*}{\Re_i}$. Based on Lemma 2, we obtain

Algorithm 2: Solution of Max-Min Rate.

Input: Given the values of the following parameters: H_U, W, K_S^B, K_M^U and σ^2.
Output: Z^* and $\mathbf{P}^*$.
Initialize $\beta = 0$, $\mathbf{P}(\beta) > 0$, $Z^* = 0$ and step size λ_μ, λ_ω and λ_H.
for $\mu = 0; \mu \le \pi; \mu = \mu + \lambda_\mu$ **do**
  for $\omega = 0; \omega \le 2\pi; \omega = \omega + \lambda_\omega$ **do**
    for $H_B = 0; H_B \le H_{max}; H_B = H_B + \lambda_H$ **do**
      Update transmit power $\mathbf{P}(\beta+1)$: $P_i(\beta+1) = F_i(\mathbf{P}(\beta))$ for each UAV i.
      Calculate the value of scale function $\phi(\mathbf{P}(\beta+1))$: $\phi(\mathbf{P}(\beta+1)) = \frac{P_{\max}}{\mathrm{m}\{P_i(\beta+1) \text{ for all } i\}}$.
      Scale transmit power $\mathbf{P}(\beta+1)$: $P_i(\beta+1) = \phi(\mathbf{P}(\beta+1))P_i(\beta+1)$ for each UAV i.
      Repeat the above update and scale operations of transmit power until convergence.
      Calculate each link rate $\Re_i$ according to (8).
      Calculate minimum rate $Z_t = \min_{i\in\Phi} \Re_i$.
      if $Z^* < Z_t$ **then**
        $Z^* = Z_t$ and $\mathbf{P}^* = \mathbf{P}$.
      end if
    end for
  end for
end for

the following fixed point equation

$$\frac{P_i^*}{Z^*} = F_i(\mathbf{P}^*). \tag{15}$$

We can express $\mathbf{F}(\mathbf{P}^*) = \mathbf{A}\mathbf{P}^*$, where $\mathbf{A}$ is a $|\Phi| \times |\Phi|$ irreducible nonnegative matrix. This means that the solution of (14) (and also (13)) equivalent to that of the conditional eigenvalue problem [35], which aims to find Z^* and $\mathbf{P}^*$ such that

$$\frac{\mathbf{P}^*}{Z^*} = \mathbf{F}(\mathbf{P}^*). \tag{16}$$

By iterating and scaling of power $\mathbf{P}$, we can obtain the optimal Z^* and $\mathbf{P}^*$ of (16). In the iterative process, $\mathbf{P}^*(\beta+1) = \mathbf{F}(\mathbf{P}^*(\beta))$, where $\mathbf{P}^*(\beta+1)$ denotes the $(\beta+1)$th iteration vector of $\mathbf{P}^*$ [36]. We use $\phi(\mathbf{P})$ denote the scale function of $\mathbf{P}$, which is defined as

$$\phi(\mathbf{P}) = \max\{x \ge 0 : xP_i \le P_{\max} \text{ for all } i\}, \tag{17}$$

where $\phi(\mathbf{P}) = 0$ only when $\mathbf{P} = 0$. Note that we select the scale function $\phi(\mathbf{P})$ such that new power vector $\phi(\mathbf{P})\mathbf{P}$ is the largest feasible solution along the direction of $\mathbf{P}$.

Therefore, we can summarize the solution of max-min rate in Algorithm 2.

Finally, we give the following Theorem presented in nonlinear Perron-Frobenius theory [35], which guarantees that the conditional eigenvalue problem of (16) has only one solution corresponding to that of transmit power vector in the Algorithm 2.

Theorem 1: For $\mathbf{F}(\mathbf{P})$, suppose the following conditions hold: (1) there exist two positive numbers a, e, and a vector $\mathbf{g} > 0$, we have $a\mathbf{g} \leqq \mathbf{F}(\mathbf{P}) \leqq e\mathbf{g}$, for each $\mathbf{P}$ satisfying the maximum power constraint in (13b); (2) for any power vectors $\mathbf{P}$ and $\mathbf{V}$, and $0 \le x \le 1$: if $x\mathbf{P} \leqq \mathbf{V}$, then $x\mathbf{F}(\mathbf{P}) \leqq \mathbf{F}(\mathbf{V})$, and for $x < 1$, if $x\mathbf{P} \le \mathbf{V}$, then $x\mathbf{F}(\mathbf{P}) \le \mathbf{F}(\mathbf{V})$. Then $\mathbf{F}(\mathbf{P})$ has the following properties:

1) There exists a unique nonzero solution Z^* at $\mathbf{P}^*$ in the conditional eigenvalue problem of (16).
2) Given any $\mathbf{P}(0) \geqq 0$ and $\phi(\mathbf{P}(0)) > 0$, the power vector $\mathbf{P}(\beta)$ converges to $\mathbf{P}^*$.

According to [35], Theorem 1 holds for $\mathbf{F}(\mathbf{P})$ that is positive and concave vector. Specially, when $\mathbf{F}(\mathbf{P})$ is concave, the Algorithm 2 can converge to a global optimal solution of the optimization problem in (14) (and also (13)). Hence, we give the following Lemma.

Lemma 3: $\mathbf{F}(\mathbf{P})$ is positive and concave.

Proof: (1) We first prove that $\mathbf{F}(\mathbf{P})$ is positive.

$$\begin{aligned} F_i(\mathbf{P}) &= \frac{P_i}{\Re_i(\mathbf{P})} \\ &= \frac{P_i}{W\log_2\left(1+\mathrm{SINR}_i(\mathbf{P},\mu,\omega,H_B)\right)} \\ &= \frac{P_i}{W\log_2\left(1+\frac{P_iK^B(\psi_i)K_M^Uh_i|L_i|^{-\alpha}}{\sum_{j\in\Phi^*,j\neq i}P_jK^B(\psi_j)K_M^Uh_j|L_j|^{-\alpha}+\sigma^2}\right)}. \end{aligned} \tag{18}$$

Calculate the partial derivative of $F_i(\mathbf{P})$ with respect to P_j under two cases of $i \neq j$ and $i = j$.

When $i \neq j$, we have

$$\frac{\partial F_i(\mathbf{P})}{\partial P_j} = \frac{P_i^2K^B(\psi_i)(K_M^U)^2h_i|L_i|^{-\alpha}K^B(\psi_j)h_j|L_j|^{-\alpha}}{W\ln(2)\log_2^2(\upsilon)\upsilon\left(\sum_{j\in\Phi^*,j\neq i}P_jK^B(\psi_j)K_M^Uh_j|L_j|^{-\alpha}+\sigma^2\right)^2} > 0, \tag{19}$$

where $\upsilon = 1 + \mathrm{SINR}_i(\mathbf{P},\mu,\omega,H_B)$.

When $i = j$, we have

$$\frac{\partial F_i(\mathbf{P})}{\partial P_j} = \frac{1}{W\log_2^2(\upsilon)}\left(\log_2(\upsilon) - \frac{\upsilon-1}{\ln(2)\upsilon}\right). \tag{20}$$

Define $f(\upsilon) = \log_2(\upsilon) - \frac{\upsilon-1}{\ln(2)\upsilon}$. Take the derivation of $f(\upsilon)$ with respect to υ, we have

$$f'(\upsilon) = \frac{\upsilon-1}{\ln(2)\upsilon^2}. \tag{21}$$

Since $\upsilon > 1$, $f'(\upsilon) > 0$, $f(\upsilon)$ is an increasing function. Since $f(1) = 0$, $f(\upsilon) > 0$ when $\upsilon > 1$. Thus, $\frac{\partial F_i(\mathbf{P})}{\partial P_j} > 0$, where $i = j$.

Since $\mathbf{F}(\mathbf{0}) = \mathbf{0}$ and $\frac{\partial F_i(\mathbf{P})}{\partial P_j} > 0$ under the two cases of $i \neq j$ and $i = j$, we obtain that $\mathbf{F}(\mathbf{P})$ is positive for $\mathbf{P} \geq 0$.

(2) We now prove that $\mathbf{F}(\mathbf{P})$ is concave function.

We utilize the result from [37]: Suppose H: $\mathbf{R}^m \to \mathbf{R}$, $\mathbf{C} \in \mathbf{R}^{m\times n}$, $\mathbf{d} \in \mathbf{R}^m$, $\mathbf{k} \in \mathbf{R}^n$ and $g \in \mathbf{R}$. Here, $\mathbf{R}^m$ denotes m

dimensional Euclidean space. Define M: $\mathbf{R}^n \to \mathbf{R}$ by

$$M(\mathbf{x}) = (\mathbf{k}^T\mathbf{x} + g)H((\mathbf{C}\mathbf{x} + \mathbf{d})/(\mathbf{k}^T\mathbf{x} + g)) \tag{22}$$

with $\mathbf{dom}(M) = \{\mathbf{x}|\mathbf{k}^T\mathbf{x} + g > 0, (\mathbf{C}\mathbf{x} + \mathbf{d})/(\mathbf{k}^T\mathbf{x} + g) \in \mathbf{dom}(H)\}$, where $\mathbf{dom}(M)$ represents the domain of function M. Then if H is concave, M is also concave.

Consider $H(z) = \frac{z}{\log_2(1+z)}$ where $z > 0$. We now prove that $H(z)$ is a concave function, which is equivalent to proving that the second derivation of $H(z)$ is less than zero.

We calculate the second derivation of $H(z)$ with respect to z.

$$\begin{aligned} H''(z) &= \frac{2z - \ln(2)(2+z)\log_2(1+z)}{\ln^2(2)(1+z)^2\log_2^3(1+z)} \\ &< \frac{2z - (2+z)\log_2(1+z)}{\ln^2(2)(1+z)^2\log_2^3(1+z)}, \end{aligned} \tag{23}$$

where since $0 < \ln(2) < 1$, (23) follows. Define $L(z) = 2z - (2+z)\log_2(1+z)$, we need to show that $L(z) < 0$.

Now, we prove that $L(z)$ is a decreasing function. Take derivation of $L(z)$, we have

$$\begin{aligned} L'(z) &= 2 - \frac{2+z}{\ln(2)(1+z)} - \log_2(1+z) \\ &< 2 - \frac{2+z}{(1+z)} - \log_2(1+z) \\ &= -\log_2(1+z) + \frac{z}{1+z}. \end{aligned} \tag{24}$$

Define $J(z) = -\log_2(1+z) + \frac{z}{1+z}$. Take the derivation of $J(z)$, then

$$J'(z) = -\frac{z}{(1+z)^2} < 0. \tag{25}$$

Thus, $J(z)$ is a decreasing function.

Since $J(0) = 0$, $J(z) < 0$ when $z > 0$. Thus, $L'(z) < 0$. We further obtain $L(z)$ is a decreasing function and $L(0) = 0$. Thus, $L(z) < 0$ when $z > 0$.

Based on $L(z) < 0$, we obtain $H''(z) < 0$ when $z > 0$. Therefore, $H(z)$ is a concave function.

We now rewrite $\mathrm{SINR_i}$ defined in (9) as

$$\begin{aligned} &\mathrm{SINR_i}(\mathbf{P}, \mu, \omega, \mathrm{H_B}) \\ &= \frac{P_i}{\sum_{j\in\Phi^*, j\neq i} \frac{P_j K^B(\psi_j) h_j |L_j|^{-\alpha}}{K^B(\psi_i) h_i |L_i|^{-\alpha}} + \frac{\sigma^2}{K^B(\psi_i) K_M^U h_i |L_i|^{-\alpha}}} \\ &= \frac{P_i}{(\mathbf{S}\mathbf{P} + \mathbf{O})_i}, \end{aligned} \tag{26}$$

where $\mathbf{S}$ is a $|\Phi^*| \times |\Phi^*|$ nonnegative matrix, each element S_{ij} of which is

$$S_{ij} = \begin{cases} 0, & \text{if i} = \text{j}, \\ \frac{P_j K^B(\psi_j) h_j |L_j|^{-\alpha}}{K^B(\psi_i) h_i |L_i|^{-\alpha}}, & \text{if i} \neq \text{j}, \end{cases}$$

and $\mathbf{O}$ is a $|\Phi^*| \times 1$ column vector, each element of which is equal to $\frac{\sigma^2}{K^B(\psi_i) K_M^U h_i |L_i|^{-\alpha}}$.

Let $m = 1$, $\mathbf{C} = \mathbf{e}_i^T$, $\mathbf{d} = \mathbf{0}$, $\mathbf{k}^T$ denote the ith row of $\mathbf{S}$, $\mathbf{x} = \mathbf{P}$, and $g = \frac{\sigma^2}{K^B(\psi_i) K_M^U h_i |L_i|^{-\alpha}}$. Here, $\mathbf{e}_i$ denotes the ith unit vector. According to the above result from [37], we obtain that $F_i(\mathbf{P})$ (and thus $\mathbf{F}(\mathbf{P})$) is concave. ■

Therefore, by the iterative process in Algorithm 2, it follows from Theorem 1 that the Algorithm 2 can converge to a global optimal solution of the optimization problem in (14) (and also (13)).

TABLE I
SYSTEM PARAMETERS

Parameters	Values
Network area	3.6×10^5 m^2
UAV density λ_U	10^{-4} UAVs/m^2
UAV height H_U	300 m
Maximum UAV transmit power P_{max}	500 mW
Number of channels N	10
Channel bandwidth W	100 MHZ
Maximum antenna height H_{max}	120 m
Antenna directivity parameter τ	1
Antenna side beam gain K_S^B	-20dB
Channel path loss exponent α	2
Channel noise power σ^2	-90 dBm

VI. NUMERICAL RESULTS

This section presents numerical results for evaluating the performances of cellular-enabled UAV swarm networks like sum rate, minimum rate and fairness index using Algorithms 1 and 2. The fairness index is used to measure the fairness of rate allocation among links [38], which is given by $\frac{(\sum_{i\in\Phi}\Re_i)^2}{|\Phi|\sum_{i\in\Phi}(\Re_i)^2}$. Here, $|\Phi|$ is the number of links as well as the number of UAVs, and the value of fairness index is in the interval [0, 1], where a small value means that the rate assignment is poor fairness. We will indicate the effect of various system parameters on the performances under the sum rate maximization and max-min rate problems. The system parameters are set in Table I, unless otherwise specified. We use PPP only to illustrate the maximum sum rate and max-min rate performances under our optimization problems and the related algorithms. Note that our proposed optimization problems and algorithms can also be applied to the situation that the locations' distributions of the UAVs are in a non-Poisson manner.

A. Effect of τ on Performances

We first explore the effect of the antenna directivity parameter τ on the three performance metrics. Fig. 2 shows the effect of τ on the sum rate under these two problems. We observe that when τ increases, the sum rate experiences first growth and then decrease under the sum rate maximization problem, while it almost keeps a constant under the max-min rate problem. We explain the reason as follows. According to formula (4), an increase of τ results in an decrease of the antenna beamwidth γ. This means that a smaller τ is associated with a bigger γ which covers a larger area where more UAVs hover. We further know from formulas (1), (2) and (3) that an increase of τ also results in the increase of the antenna main beam gain $K_M^B(\psi)$ at the BS. The phenomenon will incur the increase of more link rates. As a result, the sum rate increases when τ increases. When τ is more than a threshold, more UAVs are in the coverage area of the

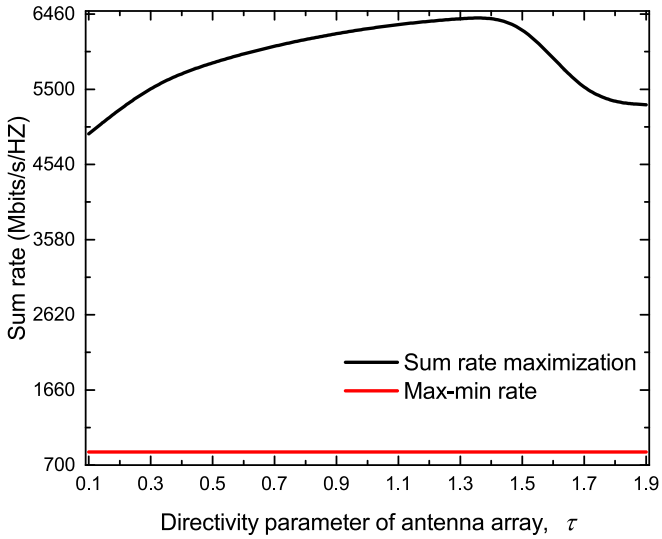

Fig. 2. Effect of τ on sum rate.

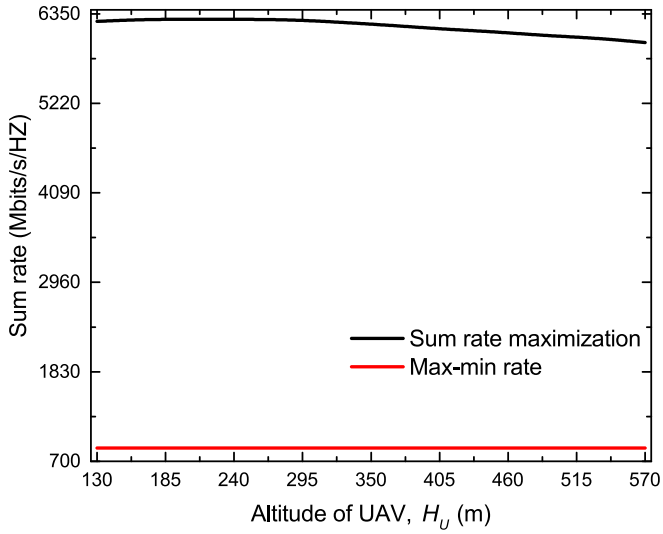

Fig. 3. Effect of H_U on sum rate.

signal from the antenna side beam with a very small gain. Thus, the sum rate decreases as τ increases. Regarding the max-min rate problem, as τ increases, each UAV can adjust its transmit power such that each link rate is the same for guaranteeing the best fairness of rate assignment among different links. Thus, the sum rate is almost unchanged under the max-min rate problem.

Regarding the effect of τ on the minimum rate, we can obtain that the minimum rate almost keeps a constant, i.e., 0.0005 Mbits/s/HZ under the sum rate maximization problem, and 19 Mbits/s/HZ under the max-min rate problem. It can be explained as follows. Under the sum rate maximization problem, more resource like transmit power is assigned to the better links while the worse links get less resource for the purpose of sum rate maximization, which leads to a very small minimum rate for each setting of τ, while under the max-min rate problem, each link has the same rate for achieving best fairness of rate assignment among different links. For the effect of τ on the fairness index, we obtain that under the sum rate maximization problem, the fairness index is approximately 0.05, which indicates that the assigned different link rates are very unfair. Under the max-min rate problem, a best fairness is achievable whose value approaches 1.

These results demonstrate that both the optimization problems are suitable for various application scenarios according to their different requirements with sum rate and fairness.

B. Effect of H_U on Performances

Fig. 3 shows the effect of UAV height H_U on the sum rate under both the optimization problems. It can be seen from Fig. 3 that as H_U increases, the sum rate increases from 6255 Mbits/s/HZ when $H_U = 130$ m to 6281 Mbits/s/HZ when $H_U = 170$ m, then keeps unchanged from $H_U = 170$ m to 250 m, and finally decreases under the sum rate maximization problem. It is due to the following reason that the increase of H_U exhibits two-fold effect on the sum rate. On the one hand, a higher H_U results in a larger coverage of antenna main beam at BS, and thus a higher antenna gain. On the other hand, it also results in a higher path loss. When H_U is low, the positive effect of the former on each link rate is more than the negative effect of the latter, and thus the sum rate increases with H_U. H_U further increases, both the former and latter have the same effect on each link rate, and thus the sum rate keeps unchanged. H_U proceeds to increase, the negative effect is greater than the positive one, and thus the sum rate decreases. Another observation from Fig. 3 illustrates that under the max-min rate problem, each link rate is the same via UAV transmit power control with the purpose of achieving fairness, and hence the sum rate is a constant.

Regarding the effect of H_U on the minimum rate, we obtain that the minimum rate almost keeps a constant, i.e., 0.0004 Mbits/s/HZ under the sum rate maximization problem, and 19 Mbits/s/HZ under the max-min rate problem. This indicates that although sum rate is very high under the sum rate maximization problem, the fairness is very poor, which is measured by fairness index almost equal to 0.05. On the contrary, the minimum rate with different settings of H_U is the same under the max-min rate problem, and corresponding fairness index is very close to 1, which demonstrates that the fairness is very good.

C. Effect of P_{max} on Performances

We proceed to explore the effect of maximum UAV transmit power P_{max} on the performance metrics. The Fig. 4 is used to show the effect of P_{max} on the sum rate. As shown in Fig. 4, when P_{max} increases, the sum rate exhibits fast increasing trend at first and then slow one. The reason behind the phenomenon can be summarized as follows. The maximum UAV transmit power increases with P_{max} for improving the sum rate performance. An increase of relative small maximum transmit power can result in an increase of each link rate, while an relative big maximum transmit power can cause the interference among links, which results in an decrease of the increasing speed for

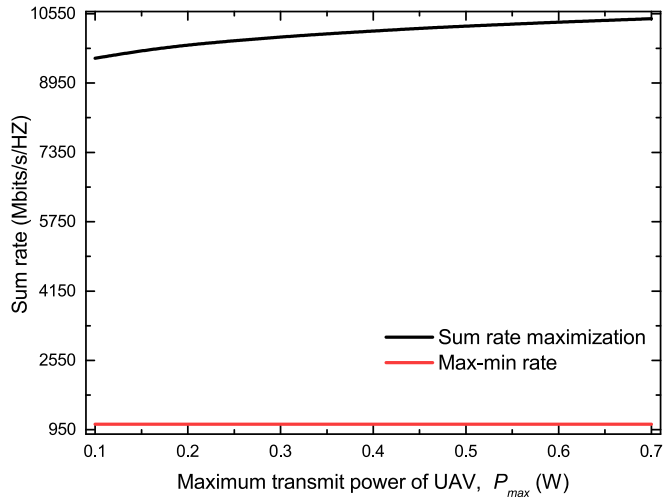

Fig. 4. Effect of P_{max} on sum rate.

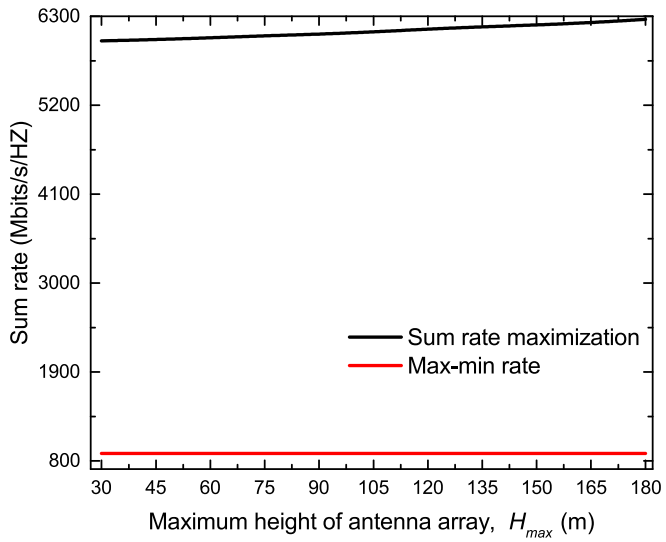

Fig. 5. Effect of H_{max} on sum rate.

each link rate. Another observation of Fig. 4 shows that under the max-min rate problem, the sum rate is a constant since each UAV can control its transmit power to achieve fair link rates.

Regarding the effect of P_{max} the minimum rate, We obtain that for the max-min rate optimization problem, the minimum rate almost keeps a constant 41 Mbits/s/HZ, while for the sum rate optimization problem, it is very close to 0. This is because the rate fairness is very poor under the sum rate optimization problem, which is measured by fairness index almost equal to 0.18. Meanwhile, the max-min rate optimization problem has very good rate fairness whose fairness index is almost equal to 1.

D. Effect of H_{max} on Performances

Finally, we explore how the effect of maximum antenna height H_{max} on the performance metrics. The results in Fig. 5 show the effect of H_{max} on the sum rate. We see that the sum rate increases with the increase of H_{max} under the sum rate maximization problem. The reason is that as H_{max} increases, we can reduce the path loss from each UAV to the antenna by increasing the optimal antenna height, which results in the increase of sum rate. Another observation of Fig. 5 indicates that the sum rate keeps a constant under the max-min rate problem. It is because each link has the same rate via UAV transmit power control for achieving the rate fairness.

Regarding the effect of H_{max} on the minimum rate, we obtain that the minimum rate almost keeps a constant. Note that the minimum rate is 0 under the sum rate maximization optimization problem. This demonstrates that the rate fairness is very poor under such an optimization problem. Thus, the fairness index is very small, which is almost equal to 0.18. We can also obtain that the max-min rate optimization problem can achieve very good rate fairness since the fairness index is very close to 1.

VII. Conclusion

This paper studied the fundamental rate performances in the cellular-enabled UAV swarm networks. We formulated them as two optimization problems subject to the constraints of UAV transmit power and the antenna parameters. Using KKT conditions and Perron-Frobenius theory, we proposed two iterative algorithms for maximizing the sum rate and minimum rate by jointly optimizing the UAV transmit power and the antenna parameters.

The numerical results reveal that we can find an optimal antenna beamwidth for achieving maximum sum rate, and increasing maximum UAV transmit power also increases sum rate under the sum rate maximization problem. However, it can also result in poor rate fairness. Contrarily, the max-min rate problem can guarantee good rate fairness with almost the same link rates, but it cannot ensure the sum rate performance. Therefore, our research is expected to satisfy different requirements with sum rate and rate fairness in future various applications of such networks. An interesting research direction is to explore the performances in the scenarios with different UAV heights in our future works.

References

[1] M. A. Ali and A. Jamalipour, "UAV placement and power allocation in uplink and downlink operations of cellular network," *IEEE Trans. Commun.*, vol. 68, no. 7, pp. 4383–4393, Jul. 2020.

[2] M. A. Ali, Y. Zeng, and A. Jamalipour, "Software-defined coexisting UAV and WiFi: Delay-oriented traffic offloading and UAV placement," *IEEE J. Sel. Areas Commun.*, vol. 38, no. 6, pp. 988–998, Jun. 2020.

[3] M. A. Ali and A. Jamalipour, "Dynamic aerial wireless power transfer optimization," *IEEE Trans. Veh. Technol.*, vol. 71, no. 4, pp. 4010–4022, Apr. 2022.

[4] Z. Chen, K. Chi, K. Zheng, Y. Li, and X. Liu, "Common throughput maximization in wireless powered communication networks with non-orthogonal multiple access," *IEEE Trans. Veh. Technol.*, vol. 69, no. 7, pp. 7692–7706, Jul. 2020.

[5] S. Hu, W. Ni, X. Wang, A. Jamalipour, and D. Ta, "Joint optimization of trajectory, propulsion, and thrust powers for covert UAV-on-UAV video tracking and surveillance," *IEEE Trans. Inf. Forensics Secur.*, vol. 16, pp. 1959–1972, 2020.

[6] N. H. Motlagh, T. Taleb, and O. Arouk, "Low-altitude unmanned aerial vehicles-based Internet of Things services: Comprehensive survey and future perspectives," *IEEE Internet of Things J.*, vol. 3, no. 6, pp. 899–922, Dec. 2016.
[7] Z. Yu, K. Chi, P. Hu, Y.-H. Zhu, and X. Liu, "Energy provision minimization in wireless powered communication networks with node throughput requirement," *IEEE Trans. Veh. Technol.*, vol. 68, no. 7, pp. 7057–7070, Jul. 2019.
[8] D.-T. Do, A.-T. Le, Y. Liu, and A. Jamalipour, "User grouping and energy harvesting in UAV-NOMA system with AF/DF relaying," *IEEE Trans. Veh. Technol.*, vol. 70, no. 11, pp. 11855–11868, Nov. 2021.
[9] K. Li, W. Ni, E. Tovar, and A. Jamalipour, "On-board deep Q-network for UAV-assisted online power transfer and data collection," *IEEE Trans. Veh. Technol.*, vol. 68, no. 12, pp. 12215–12226, Dec. 2019.
[10] X. Zhang and L. Duan, "Fast deployment of UAV networks for optimal wireless coverage," *IEEE Trans. Mobile Comput.*, vol. 18, no. 3, pp. 588–601, Mar. 2019.
[11] Y. Zeng and R. Zhang, "Energy-efficient UAV communication with trajectory optimization," *IEEE Trans. Wireless Commun.*, vol. 16, no. 6, pp. 3747–3760, Jun. 2017.
[12] Y. Zeng, X. Xu, and R. Zhang, "Trajectory design for completion time minimization in UAV-enabled multicasting," *IEEE Trans. Wireless Commun.*, vol. 17, no. 4, pp. 2233–2246, Apr. 2018.
[13] V. V. Chetlur and H. S. Dhillon, "Downlink coverage analysis for a finite 3-D wireless network of unmanned aerial vehicles," *IEEE Trans. Commun.*, vol. 65, no. 10, pp. 4543–4558, Oct. 2017.
[14] Y. Zeng, R. Zhang, and T. J. Lim, "Throughput maximization for UAV-enabled mobile relaying systems," *IEEE Trans. Commun.*, vol. 64, no. 12, pp. 4983–4996, Dec. 2016.
[15] C. Shen, T.-H. Chang, J. Gong, Y. Zeng, and R. Zhang, "Multi-UAV interference coordination via joint trajectory and power control," *IEEE Trans. Signal Process.*, vol. 68, pp. 843–858, 2020.
[16] C. You and R. Zhang, "3D trajectory optimization in Rician fading for UAV-enabled data harvesting," *IEEE Trans. Wireless Commun.*, vol. 18, no. 6, pp. 3192–3207, Jun. 2019.
[17] H. He, S. Zhang, Y. Zeng, and R. Zhang, "Joint altitude and beamwidth optimization for UAV-enabled multiuser communications," *IEEE Commun. Lett.*, vol. 22, no. 2, pp. 344–347, Feb. 2018.
[18] M. Hua, L. Yang, Q. Wu, and A. L. Swindlehurst, "3D UAV trajectory and communication design for simultaneous uplink and downlink transmission," *IEEE Trans. Commun.*, vol. 68, no. 9, pp. 5908–5923, Sep. 2020.
[19] Q. Wu and R. Zhang, "Common throughput maximization in UAV-enabled OFDMA systems with delay consideration," *IEEE Trans. Commun.*, vol. 66, no. 12, pp. 6614–6627, Dec. 2018.
[20] Y. Zeng, J. Xu, and R. Zhang, "Energy minimization for wireless communication with rotary-wing UAV," *IEEE Trans. Wireless Commun.*, vol. 18, no. 4, pp. 2329–2345, Apr. 2019.
[21] A. A. Nasir, H. D. Tuan, T. Q. Duong, and H. V. Poor, "UAV-enabled communication using NOMA," *IEEE Trans. Commun.*, vol. 67, no. 7, pp. 5126–5138, Jul. 2019.
[22] Q. Wu, Y. Zeng, and R. Zhang, "Joint trajectory and communication design for multi-UAV enabled wireless networks," *IEEE Trans. Wireless Commun.*, vol. 17, no. 3, pp. 2109–2121, Mar. 2018.
[23] H. Wu, X. Tao, N. Zhang, and X. Shen, "Cooperative UAV cluster assisted terrestrial cellular networks for ubiquitous coverage," *IEEE J. Sel. Areas Commun.*, vol. 36, no. 9, pp. 2045–2058, Sep. 2018.
[24] S. Zhang, Y. Zeng, and R. Zhang, "Cellular-enabled UAV communication: A connectivity-constrained trajectory optimization perspective," *IEEE Trans. Commun.*, vol. 67, no. 3, pp. 2580–2604, Mar. 2019.
[25] W. Mei and R. Zhang, "Cooperative downlink interference transmission and cancellation for cellular-connected UAV: A divide-and-conquer approach," *IEEE Trans. Commun.*, vol. 68, no. 2, pp. 1297–1311, Feb. 2020.
[26] S. Zhang, H. Zhang, B. Di, and L. Song, "Cellular UAV-to-X communications: Design and optimization for multi-UAV networks," *IEEE Trans. Wireless Commun.*, vol. 18, no. 2, pp. 1346–1359, Feb. 2019.
[27] W. Mei, Q. Wu, and R. Zhang, "Cellular-connected UAV: Uplink association, power control and interference coordination," *IEEE Trans. Wireless Commun.*, vol. 18, no. 11, pp. 5380–5393, Nov. 2019.
[28] Y. Li, G. Feng, M. Ghasemiahmadi, and L. Cai, "Power allocation and 3-D placement for floating relay supporting indoor communications," *IEEE Trans. Mobile Comput.*, vol. 18, no. 3, pp. 618–631, Mar. 2019.
[29] B. Yang, T. Taleb, Z. Wu, and L. Ma, "Spectrum sharing for secrecy performance enhancement in D2D-enabled UAV networks," *IEEE Netw.*, vol. 34, no. 6, pp. 156–163, Nov./Dec. 2020.
[30] B. Yang, T. Taleb, Y. Fan, and S. Shen, "Mode selection and cooperative jamming for covert communication in D2D underlaid UAV networks," *IEEE Netw.*, vol. 35, no. 2, pp. 104–111, Mar./Apr. 2021.
[31] P. Jankowski-Mihulowicz, W. Lichon, and M. Weglarski, "Numerical model of directional radiation pattern based on primary antenna parameters," *Int. J. Electron. Telecommun.*, vol. 61, no. 2, pp. 191–197, Jul. 2015.
[32] B. Yang, T. Taleb, Y. Shen, X. Jiang, and W. Yang, "Performance, fairness, and tradeoff in UAV swarm underlaid mmWave cellular networks with directional antennas," *IEEE Trans. Wireless Commun.*, vol. 20, no. 4, pp. 2383–2397, Apr. 2021.
[33] A. Goldsmith, *Wireless Communications*. Cambridge, U.K.: Cambridge Univ. Press, 2005.
[34] C. A. Balanis, *Antenna Theory: Analysis and Design*, 3rd ed.Hoboken, NJ, USA: Wiley-Interscience, 2005.
[35] U. Krause, "Perron's stability theorem for nonlinear mappings," *J. Math. Econ.*, vol. 15, no. 3, pp. 275–282, Mar. 1986.
[36] A. Berman and R. J. Plemmons, *Nonnegative Matrices in the Mathematical Sciences*. New York, NY, USA: Academic Press, 1979.
[37] S. Boyd and L. Vanderberghe, *Convex Optimization*. Cambridge, U.K.: Cambridge Univ. Press, 2004.
[38] T. Taleb, N. Kato, and Y. Nemoto, "An explicit and fair window adjustment method to enhance TCP efficiency and fairness over multihops satellite networks," *IEEE J. Sel. Areas Commun.*, vol. 22, no. 2, pp. 371–387, Feb. 2004.

Bin Yang received the Ph.D. degree in systems information science from Future University Hakodate, Hakodate, Japan, in 2015. He is currently a Professor with the School of Computer and Information Engineering, Chuzhou University, Chuzhou, China. His research interests include unmanned aerial vehicle networks, cyber security, and Internet of Things.

Yongchao Dang received the B.S. degree from the School of Computer Science, Northwestern Polytechnical University, Xi'an, China, in 2016, and the M.S. degree from the School of Computer Science and Technology, Xidian University, Xi'an, China, in 2019. He is currently working toward the Doctoral degree with the School of Electrical Engineering, Aalto University, Espoo, Finland. His research interests include unmanned aerial vehicles, machine learning, wireless communication, and network security.

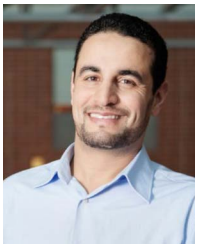

Tarik Taleb received the B.E. degree in information engineering (with distinction), and the M.Sc. and Ph.D. degrees in information sciences from Tohoku University, Sendai, Japan, in 2001, 2003, and 2005, respectively.

He is currently a Professor with the Centre for Wireless Communications, Networks and Systems Unit, Faculty of Information Technology and Electrical Engineering, The University of Oulu, Oulu, Finland. He is the Founder and Director of the MOSA!C Lab. Between October 2014 and December 2021, he was a Professor with the School of Electrical Engineering, Aalto University, Espoo, Finland. Prior to that, he was a Senior Researcher and 3GPP Standards Expert with NEC Europe Ltd., Heidelberg, Germany. Before joining NEC and till March 2009, he was an Assistant Professor with the Graduate School of Information Sciences, Tohoku University, Sendai, Japan, in a lab fully funded by KDDI, the second largest mobile operator in Japan. From October 2005 to March 2006, he was a Research Fellow with the Intelligent Cosmos Research Institute, Sendai, Japan. His research interests include telco cloud, network softwarization and network slicing, AI-based software defined security, immersive communications, mobile multimedia streaming, and next generation mobile networking. He has been also directly engaged in the development and standardization of the Evolved Packet System as a Member of 3GPP.s System Architecture working group 2.

Dr. Taleb was the General Chair of the 2019 edition of the IEEE Wireless Communications and Networking Conference (WCNC.19) held in Marrakech, Morocco. He was the Guest Editor in Chief of the IEEE JSAC Series on Network Softwarization and Enablers. He was on the Editorial Board of the IEEE TRANSACTIONS ON WIRELESS COMMUNICATIONS, *IEEE Wireless Communications Magazine*, IEEE JOURNAL ON INTERNET OF THINGS, IEEE TRANSACTIONS ON VEHICULAR TECHNOLOGY, IEEE COMMUNICATIONS SURVEYS AND TUTORIALS, and a number of Wiley journals. Till December 2016, he was the Chair of the Wireless Communications Technical Committee, the largest in IEEE ComSoC. He was also the Vice Chair of the Satellite and Space Communications Technical Committee of IEEE ComSoc during 2006–2010. He is the recipient of the 2021 IEEE ComSoc Wireless Communications Technical Committee Recognition Award in December 2021 and the 2017 IEEE ComSoc Communications Software Technical Achievement Award in December 2017 for his outstanding contributions to network softwarization. He is also the co-recipient of the 2017 IEEE Communications Society Fred W. Ellersick Prize in May 2017, 2009 IEEE ComSoc Asia-Pacific Best Young Researcher Award in June 2009, 2008 TELECOM System Technology Award from the Telecommunications Advancement Foundation in March 2008, 2007 Funai Foundation Science Promotion Award in April 2007, 2006 IEEE Computer Society Japan Chapter Young Author Award in December 2006, Niwa Yasujirou Memorial Award in February 2005, and Young Researcher's Encouragement Award from the Japan chapter of the IEEE Vehicular Technology Society (VTS) in October 2003. Some of his research work have been also awarded best paper awards at prestigious IEEE-flagged conferences.

Shikai Shen received the B.S. degree from Yunnan Normal University, Kunming, China, in 1984, and the M.S. degree from Yunnan University, Kunming, China, in 2003. He is currently a Professor with Kunming University, Kunming, China. His research interests include wireless sensor networks, cyber security, and Internet of Things.

Xiaohong Jiang received the B.S., M.S., and Ph.D. degrees from Xidian University, Xi'an, China, in 1989, 1992, and 1999, respectively. He is currently a Full Professor with Future University Hakodate, Hakodate, Japan. Before joining Future University, he was an Associate Professor with Tohoku University, Sendai, Japan, from February 2005 to March 2010. He has authored or coauthored more than 300 technical papers at premium international journals and conferences, which include more than 70 papers published in top IEEE journals and top IEEE conferences, such as IEEE/ACM TRANSACTIONS ON NETWORKING, IEEE JOURNAL OF SELECTED AREAS ON COMMUNICATIONS, IEEE TRANSACTIONS ON PARALLEL AND DISTRIBUTED SYSTEMS, and IEEE INFOCOM. His research interests include computer communications networks, mainly wireless networks and optical networks, network security, and routers/switches design.